



SEGMENTATION OF THE INDISTINCT MISTY IMAGE USING AN EFFICIENT ALGORITHM AND RESTORATION OF THE IMAGE AND IDENTIFICATION OF THE FACIAL FEATURES OF HUMANS

P. Vijay Kumar¹, Indumathi Subramaniam²

¹M.Tech, Asst. Professor, ²M.Tech, Student,

VR Siddhartha Engineering College, Kanuru, Vijayawada, Krishna District, Andhra Pradesh.

Abstract

A snap that is clicked for any purpose always needn't be the perfectly expected snap and could contain unwanted faults in it too. Reasons that cause the unnecessary disturbances in the photo could be because of irregular or accidental shake of camera, object motion blur inadequately focussed glazed image also causes blur that causes faults with the clicked photo. So an unintentional blur decreases the visual effectiveness of the image needs to be enhanced for any information retrieval from the image. Here partially focussed blur is considered as a problem in which the blurred region needs to be segmented and restored. We consider local binary pattern to be the sharpness metric and develop an algorithm for segmentation. The sharpness metric defines that the most of image regions in obscure regions have few neighbouring binary patterns when compared with those in sharp regions. Hence the following stage is magnify and restore the inadequately focussed image by a method of using optimization and blur map. Once the inadequately focussed image is restored there is also a possibility identifying the facial features if the image has straight facing human facing the camera. So by using the Viola Jones algorithm we could detect the face and its respective features. The above proposed methods have been tested on many inaccurately focussed images which has at least one human face in the image. The proposed and tested method has better

accuracy, quick time lapse over other methods.

Keywords: Inaccurately focussed, segmentation, image restoration, facial feature detection

1. INTRODUCTION

The digital pictures that are clicked by any camera tends to invite some unwanted disturbances that decreases the image quality. Blur detection and estimation solves many problems in digital image processing, computer vision, computer image. A set of images of the same scene is captured using multiple focus settings. In an image to estimate an out of focus blur is challenging as the corresponding PSFs are spatially varying and the corresponding puff cannot be represented by any global descriptor. A spatially varying inaccurately focussed PSFs for a given camera can be pre-calibrated and described through a simple model. For an image we consider to experiment with the 2D map of the scale parameter the misty blur map, which indicates the level of local blur at each pixel. The inaccurately blur level is very closely related to the depth of the scene so a blur map also provides important information for depth estimation. The computation of depth information generally requires two photos of the same scene taken at the same time, but from slightly different vantage points.

2. LITERATURE SURVEY

Singh Karla et al [1] proposed in their tested method an algorithm is for the performance of segmentation that creates the boundaries of the

object under observation. Segmentation of the considered image is performed to fulfil the purpose of separating the focused object from the blurred background. The uniformly blurred image is convolved with the focused part of the image. Then deconvolution is performed on the image in order to achieve a more clearer output image. The steps in the algorithm includes the consideration of image, segmentation by adaptive thresholding of the image, blur kernel estimation followed by convolution and deconvolution

Zhu et al [2] found that the sub-area of a window with the smallest blur size tends to dominate the probability analysis because the sub-area contributes more power per pixel to the power spectrum. Therefore the sharp areas would be enlarged by the radius of the analysis window in an image produced without the coherence labelling step. So to rely on the coherence labelling is snap the boundary to closest colour boundary in the underlying image, that is where usually the actually depth discontinuity lies. Certain conditions where this fails as in the cases of gradually changing blur, or in cases where there is not a good colour boundary at the depth discontinuity. When we observe the step of coherence labelling the afore mentioned correcting influence has to set the parameter to a significant value. Thereby it could cause a slight over smoothing and declares that the blur values takes discrete steps in areas where the blur changes continuously. The jaggedness of the contours in the same figure is due to uncertainty present in the statistical computation. Even though the results appear to be quite good there are certain problems due to the increased energy that follows a serpentine contour.

3. PROPOSED METHOD

In our method we use local binary patterns which are computationally efficient texture descriptor.

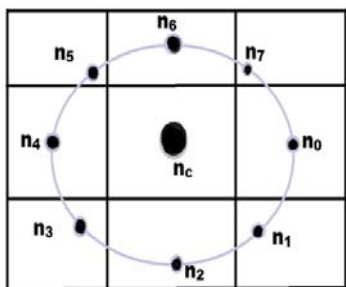


Figure 1. 8 bit LBP with n_c as the center pixel and the rest are neighbouring pixels

The LBP of a pixel is given by

$$LBP_{P,R}(x_c,y_c) = \sum_{i=0}^{P-1} S(n_p - n_c) \times 2^i$$

Here $S(x) = 1 |x| \geq T_{LBP}$
 And $S(x) = 0 |x| < T_{LBP}$ (3.1)

Where c is the central pixel values (x_c,y_c) and n_p corresponds to the P neighbouring pixels. Local binary pattern considers a centre pixel value and then identifies all pixels with luminance less than that of the centre pixel luminance and the remaining pixels are greater than or equal to that of the centre pixel luminance value and we must unroll the circular pattern to get the local binary pattern label and thus we get a binary value which we convert into a decimal value. But uniform local binary pattern is not robust to rotation and the solution to solve it is to use a Fourier transform of histogram.

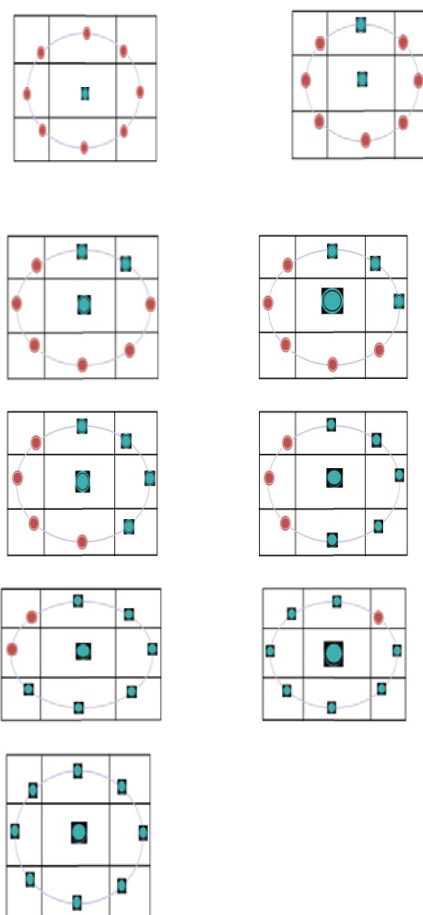


Figure 2. Uniform rotationally invariant LBP

The LBP metric of our method could be given by the following equation as :

$$m_{LBP} = \frac{1}{N} \sum_{i=6}^9 n(LBP_{8,1}^{riu2} i) \quad (3.2)$$

Where $n(LBP_{8,1}^{riu2} i)$ is the number of rotation invariant uniform 8-bit LBP pattern of type i , N is the total number of pixels in the selected local region which tends to normalize the metric so that $m_{LBP} \in [0,1]$.

OUT OF FOCUS BLUR SEGMENTATION ALGORITHM

Here the algorithm follows the steps as in the figure 3 and we need to give the inaccurately focussed images as input.

Multi scale sharpness map generation

Multi-scale sharpness maps are generated using m_{LBP} . The sharpness metric is computed for a local patch about each image pixel. Sharpness maps are constructed at three scales where scale refers to local patch size. By using an integral image, sharpness maps may be computed in constant time per pixel for a fixed P and R .

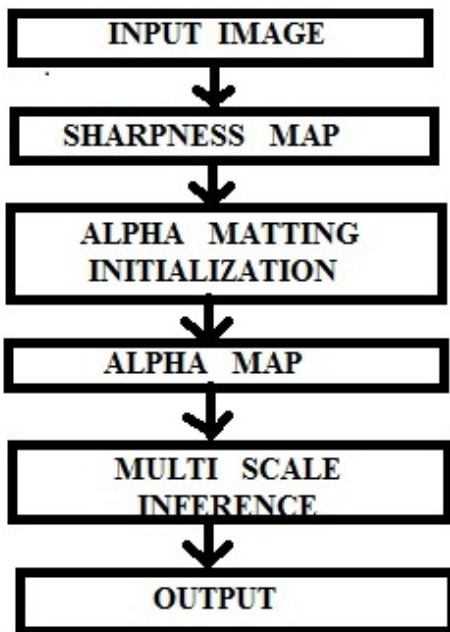


Figure 3. The steps for the blur segmentation algorithm

Alpha Matting Initialization

Alpha matting decomposes an image into foreground and background. The image formation model can be expressed as

$$I(x,y) = \alpha_{x,y} F(x,y) + (1 - \alpha_{x,y}) B(x,y)$$

$$\begin{aligned} \text{mask}^s(x,y) &= 1 \text{ if } m_{LBP}(x,y) > T_{m1} \\ \text{mask}^s(x,y) &= 0 \text{ if } m_{LBP}(x,y) < T_{m1} \\ \text{mask}^s(x,y) &= m_{LBP}(x,y), \text{ otherwise} \end{aligned} \quad (3.3)$$

Where the alpha matte, $\alpha_{x,y}$ is the opacity value on pixel position (x,y) . Alpha matting requires mark a known foreground as $\alpha = 1$ and background pixels as $\alpha = 0$. Assuming the “foreground” as “sharp” and background as “blurred” we initialize the alpha matting process by applying a double threshold to the sharpness maps computed in the previous step.

Alpha Map Computation

The α -map was solved by solving

$$E(\alpha) = \alpha^T L \alpha + \lambda (\alpha - \tilde{\alpha})^T (\alpha - \tilde{\alpha}) \quad (3.4)$$

Where α is the vectorized α -map, $\tilde{\alpha} = \text{mask}^i(x,y)$ is vectorized initialization alpha maps from the previous step, and L is the matting laplacian matrix. The before equal to term is the regulation term that ensures smoothness, and the after equal to term is the data fitting term that encourages similarity to. The final alpha map at each scale is taken as $s=1,2,3$.

Multi Scale Inference

After determining the alpha map at three different scales, a multi-scale graphical model was adopted to make the final decision. The total energy on the graphical model is expressed as

$$\begin{aligned} E(h) = & \sum_i i \sum_{s=1}^3 |h_i^s - \hat{h}_i^s| + \\ & \beta (\sum_i i \sum_{j \in N_i^s} \sum_{s=1}^3 |h_i^s - h_j^s| + \sum_i i \sum_{s=1}^2 |h_i^s + h_i^{s+1}|) \end{aligned} \quad (3.5)$$

Here $\hat{h}_i^s = \alpha_i^s$ is the alpha map for scale s at pixel location i that was computed in the previous step, and h_i^s is the sharpness to be inferred. The right hand side term is the unary term which is the cost of assigning sharpness value h_i^s to pixel i in scale s . The second is the pairwise term that enforces smoothness in the same scale and across different scales. The weight is given by β . So the output of the algorithm is that the misty regions are black in

colour and the clearer regions are white in colour.

Image restoration

There is a necessity to get blur map taking local contrast prior and the guided filter. Then by using image blur minimising method with L1-2 optimization a better image quality is obtained. In the final step, we adopt the scale selection to select the deblurred pixels to fill in the final all-in-focus output.

Blur map generation

A latent edge signal $l(x)$ is considered and we model it as

$$l(x) = A \cdot U(x) + B \quad (3.6)$$

Here A is the amplitude, B is the offset, $u(x)$ is the step function, the edge is located at $x=0$. If the edge signal $l(x)$ suffers from indistinct blur we could approximate the blurry signal $b(x)$ as the convolution as the following

$$b(x) = l(x) \otimes g(x, \sigma) \quad (3.7)$$

where $g(x, \sigma)$ is a Gaussian function with standard deviation σ . In order to extract the blur scale σ we need to use the local contrast prior [3] and modify using the edge properties [5]. Following the previous equations, we can obtain the gradient of the blurry edge and then substitute it into $LC(x)$.

$$\nabla b(x) = \nabla(l(x) \otimes g(x, \sigma)) = A \cdot G(x, \sigma)$$

$$LC(x) = \frac{\max |\nabla b(x^1)|}{\max b(x^1) - \min b(x^1)} \approx \frac{1}{\sqrt{2\pi}\sigma} \max |\exp(-\frac{x^2}{2\sigma^2})| \quad (3.9)$$

Here x^1 is the neighbourhood of x . Therefore to obtain the required blur map as a starting step for the image retrieval we consider the following equation

$$\sigma(x, y) = \frac{1}{\sqrt{2\pi}LC(x,y)} = \frac{0.3989}{LC(x,y)} \quad (3.10)$$

where $LC(x,y) = \frac{\max |\nabla b(x^1,y^1)|}{\max b(x^1,y^1) - \min b(x^1,y^1)}$ and (x^1, y^1) is the neighbourhood of (x,y) within a local window.

Image deblurring using L1 -2 optimization

After generating the blur map, we make the image clearer by using L1-2 optimization to obtain the deblurred images for focussed clear image reconstruction. Consider the non focussed part in the image be the blurry image, G_σ

represents the Gaussian blurring operator with blur scale σ , l_σ is the corresponding deblurred $n \times n$ gray scale image and r is the additive noise

$$b = G_\sigma l_\sigma + r \quad (3.11)$$

Here b is the blurry input and the term g_σ is supposed to be pre determined.

$$\min = \frac{\mu}{2} \|G_\sigma l_\sigma - b\|_2^2 + \alpha \cdot \sum_{i=1}^n |D_i l_\sigma| + (1 - \alpha) \quad (3.12)$$

where $D_i l_\sigma$ denotes the discrete gradient of l_σ at pixel i , and $\sum \|D_i l_\sigma\|^2$ is the TV regularizer of l_σ is the Tikhonov-like regularizer. And μ is a parameter and $0 < \alpha < 1$. For a fixed l_σ , only the middle two term related to w_i are separable with respect to w_i we substitute as

$$\min \|w_i\| + \frac{\beta}{2} \sum_{i=1}^{n^2} \|w_i - D_i l_\sigma\|_2^2 \quad (3.13)$$

for which the unique solver is given using matrix calculus by

$$w_i = \max \{ \|D_i l_\sigma\| - \frac{1}{\beta}, 0 \} \frac{D_i l_\sigma}{\|D_i l_\sigma\|} \quad (3.14)$$

where $i = 1, 2, \dots, n^2$ and the convention $(0/0) = 0$. If w_i can be fixed then we could obtain l_σ . Assuming l_σ is under the periodic boundary condition we have D_i and $G_\sigma^T G_\sigma$ are all block circulant. Therefore by utilizing 2D discrete fourier transform F we need to replace the huge matrix calculation. Using the convolution theorem of Fourier transforms, we can obtain l_σ from the digital filter. In the alternating minimizing algorithm we can initialize $b = l_\sigma$ and iteratively compute ω for a fixed l_σ and vice versa. Until the minimizing penalty function reaches its convergence, we can obtain the final deblurred image l_σ . Using different blur scales, we can obtain N deblurred image candidates $\{ l_{\sigma_1}, l_{\sigma_2}, l_{\sigma_3}, \dots, l_{\sigma_n} \}$ for image reconstruction.

Scale selection for image reconstruction

To rearrange the all in focus image we use

$$l^*(x, y) = \sum_{x,y} l_{\sigma^*(x,y)}(x, y) \quad (3.15)$$

Where $\sigma^*(x, y)$ is the biggest quantized blur scale close to $\sigma(x, y)$. As $\sigma^*(x, y) \leq \sigma(x, y)$ we can suppress the ringing artefacts which are caused by non regularity.

Facial detail identification in the image

The impressive points about Viola Jones algorithm is its a seminal approach to real-time object detection Even though the training is slow

detection is very fast. Vital points include integral images for fast feature evaluation, boosting for feature selection, attentional cascade for fast rejection of non-face windows. The image features are evaluated or identified by using of the rectangular filters and its value is calculated by taking the summation of pixels in white areas subtracted from the summation of pixels in the dark areas. We need to do the fast computation with integral images by computing the that is the sum of the pixel values above and to the left of (x,y), inclusive . This can be computed in one pass through the image.

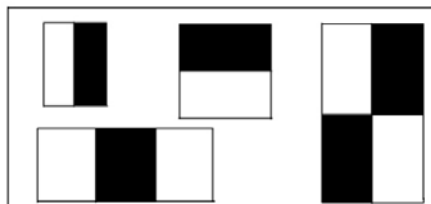


Figure 4. Image features rectangular filters

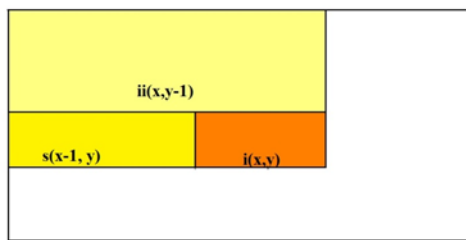


Figure 5. Computation of the integral image

When we need to compute the sum within a rectangle then lets consider A,B,C,D as the values of the integral image at the corners of a rectangle. The sum of original image values within the rectangle can be computed as $sum = A - B - C + D$ so we need only three additions are required for any size of rectangle.

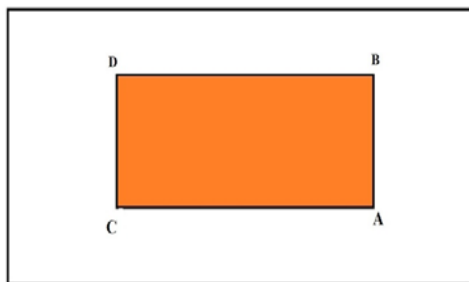


Figure 6. Computation of sum within the rectangle

For feature selection we consider a 24x24 detection region and the number of possible rectangle features is approximately equal to 1,60,000.

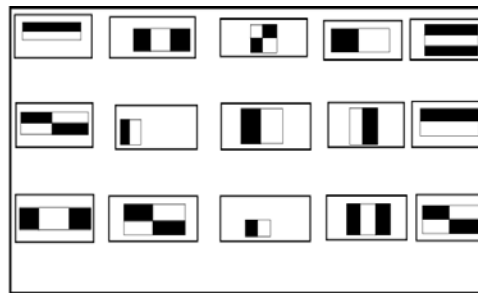


Figure 7. Feature selection

At the testing time it is impractical to evaluate the entire feature set. So we need a good classifier using just a small subset of all possible features. Thus the exact formulas for re-weighting and combining weak learners depend on the particular boosting scheme for example like the AdaBoost. While using boosting for face detection we define weak learners based on rectangle features for each round of boosting and evaluate each rectangle filter on each example and select best threshold for each filter and select best filter or threshold combination. After many steps of processing the number of sub-windows would reduced radically. For K stages of cascading with each stage having f_i as the false positive rate, the overall false positive rate for the cascade is

$$F = \prod_{i=1}^K f_i$$

the overall detection rate is

$$D = \prod_{i=1}^K d_i$$

To keep F very low and D very high, for each stage the goal is to have very high detection rate (close to 100%), but moderate false positive rate (say, 30%). In the case of the cascaded classifier as shown below

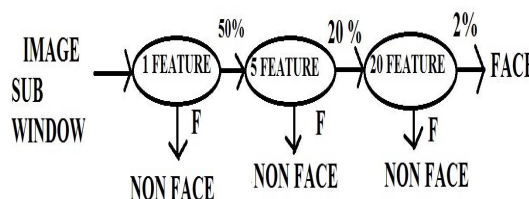


Figure 8. Chain classifiers in attentional cascade

SIMULATION RESULTS



Figure 9. Segmentation of the clear and inaccurately focused image regions.



Figure 10. Restored out of focus image with a visibly clearer background.



Figure 11. Face detected in the deblurred image.



Figure 12. Mouth detected in the clearer image.



Figure 13. Nose detected in the clearer image.



Figure 14. Eyes detected in the clearer image.

5. CONCLUSION

As seen by the above methods described and the results as shown an easy yet efficient method for out of focus image segmentation is described and not leaving the segmented region as a dark and lighter one we even restore the out of focus image by using the L1-2 optimization and further detect the facial features such as the mouth, nose, eyes along with the face detection by using the Viola Jones algorithm. Our sharpness metric measures sure LBP patterns in the native neighbourhood so its efficiency is enforced by integral pictures. If combined with period matting algorithms, such as GPU implementations of world matting, our methodology would have acquires speed advantage over the other defocus segmentation algorithms. Hence the above described methods are quite accurate and faster when compared to the other existing methods and achieves better results than the previously used methods for detection, restoration.

REFERENCES

1) Image deblurring using segmentation by Gusharanjeet Singh Kalra, Johar Aditi, Johar.A, International Journal of Computer Applications (0975 – 8887), Volume 93 – No.17, May 2014.

- 2) Estimating Spatially Varying Defocus Blur from A Single Image Xiang Zhu, Student Member, IEEE, Scott Cohen, Member, IEEE, Stephen Schiller, Member, IEEE, and Peyman Milanfar, Fellow, IEEE
- 3) Blurred image region detection and classification by Bol Su, Shijian Lu, Chew Lim Tan, School of Computing, National University of Singapore Computing 1(COM1).
- 4) Higher order image co segmentation by Wenguan Wang and Jianbing Shen, Senior Member, IEEE, IEEE transactions on multimedia, vol. 18, no. 6, June 2016.
- 5) Image partial blur detection and classification Renting Liu, Zhaorong Li, Jiaya Jia department of computer science and engineering the Chinese University of Hong Kong.
- 6) Image deblurring from blurred images Sonu Jain, Akhilesh Dubey, Diljeet Singh Chundawat, Prabhat Kumar Singh, International Journal of Advanced Research in Computer Science & Technology.
- 7) S. Bae and F. Durand, "Defocus magnification," *Comput. Graph. Forum*, vol. 26, no. 3, pp. 571–579, 2007.
- 8) K. Bahrami, A. C. Kot, and J. Fan, "A novel approach for partial blur detection and segmentation," in *Proc. IEEE Int. Conf. Multimedia Expo (ICME)*, Jul. 2013, pp. 1–6.
- 9) J. Bardsley, S. Jefferies, J. Nagy, and R. Plemmons, "A computational method for the restoration of images with an unknown, spatially varying blur," *Opt. Exp.*, vol. 14, no. 5, pp. 1767–1782, 2006.
- 10) A. Buades, B. Coll, and J.-M. Morel, "A nonlocal algorithm for image denoising," in *Proc. IEEE Comput. Soc. Conf. Comput. Vis. Pattern Recognit. (CVPR)*, vol. 2, Jun. 2005, pp. 60–65.
- [11] A. Chakrabarti, T. Zickler, and W. T. Freeman, "Analyzing spatially-varying blur," in *Proc. IEEE Conf. Comput. Vis. Pattern Recognit. (CVPR)*, Jun. 2010, pp. 2512–2519.
- [12] S. Dai and Y. Wu, "Removing partial blur in a single image," in *Proc. IEEE Conf. Comput. Vis. Pattern Recognit. (CVPR)*, Jun. 2009, pp. 2544–2551.